# Enhancement of the absorption of a backed rigid frame porous layer using a 2-dimensional periodic multi-irregularities rigid backing

Bruno Brouard, Jean-Philippe Groby, Olivier Dazel, Benoit Nennig, Luc Kelders

ACOUSTICS 2012

# Enhancement of the absorption of a backed rigid frame porous layer using a 2-dimensional periodic multi-irregularities rigid backing

B. Brouard[a], J.-P. Groby[a], O. Dazel[a], B. Nennig[b] and L. Kelders[c]

[a]Laboratoire d'acoustique de l'université du Maine, Bât. IAM - UFR Sciences Avenue Olivier Messiaen 72085 Le Mans Cedex 9
[b]Laboratoire d'Ingénierie des Systèmes Mécaniques et des MAtériaux, Supméca - 3, rue Fernand Hainaut - 93407 St Ouen Cedex
[c]Laboratory of Acoustics and Thermal Physics, KULeuven, B-3001 Heverlee, Belgium
bruno.brouard@univ-lemans.fr

This work was initially motivated by a design problem for the absorption of sound connected to the determination of the optimal profile of a discontinuous spatial distribution of porous materials and of the geometric properties. It extend the work proposed in [1], to a 3D problem involving a 2 D grating. The acoustic properties of a medium resistivity porous layer backed by a rigid plate containing periodic rectangular irregularities, creating a multi-component diffraction gratings is investigated. Numerical and experimental results show that the structure possesses total absorption peaks at the frequencies of the modified mode of the layer and/or of the trapped mode associated to the irregularities, when designed as proposed. These results is explained by an analysis of the acoustic response of the whole structure and especially by the modal analysis of the configuration. When more than one irregularity per spatial period is considered, additional higher frequency peaks are observed.

# 1 Introduction

This work was initially motivated by a design problem for the absorption of sound connected to the determination of the optimal profile of a discontinuous spatial distribution of porous materials and of the geometric properties. Porous materials (foam) suffer from a lack of absorption at low frequencies, when compared to the values at higher frequencies. The usual way to solve this problem is by multi-layering [2, 3, 4]. The purpose of the present article is to investigate an alternative to multi-layering by considering periodic irregularities of the rigid plate on which a porous sheet is attached, thus creating a diffraction grating and therefore extending previous works[1] already conducted in 2-dimensional configurations to 3-dimensional ones.

The influence of the irregularity was previously investigated by use of the multi-modal method in[1], by considering periodic rectangular air-filled irregularities of the rigid plate on which porous sheets are often attached in 2-dimensional configurations. This was found to lead, in the case of one irregularity per spatial period, to a total absorption peak associated with the excitation of the fundamental modified mode of the backed layer. This mode is excited thanks to the surface grating. Such configurations have been widely studied in room acoustics whereby irregularities are introduced to the walls in a space to enhance the diffusion and absorption effects[5], but the considered phenomenon is mostly related to resonance of the irregularities. Other works related to surface irregularities were carried out, notably related to local resonances associated with fractal irregularities[6, 7]. In addition, the influence of the addition of a volumic heterogeneity on absorption of porous layers was previously investigated by use of the multipole method, by embedding a periodic set of high-contrast inclusions, whose size is not small compared with the wavelength, in a macroscopically-homogeneous porous layer backed by a rigid flat backing in [8] or by periodic irregular rigid backing in [9], whose thickness and weight are relatively small. It was found, that the structure possesses almost total absorption peaks, associated with trapped modes that trap the energy between the heteorogeneities and the rigid plate and associated with the resonances of the irregularity that trap the energy inside the irregularity, below the so-called quarter wavelength resonance of the plate, when irregularities and heterogeneities are correctly designed.

In this paper, the effect of a 3-dimensional periodic irregularity of the rigid backing on which a porous slab is attached is investigated theoretically, numerically and experimentally.

# 2 Formulation of the problem

## 2.1 Description of the configuration

The 3D scattering problem is shown in Fig.1. Before the addition of the structured backing, the layer is a porous material $M^{[1]}$ saturated by air (e.g., a foam) which is modelled as an equivalent fluid using the Johnson-Champoux-Allard model. The upper and lower flat and mutually-parallel boundaries of the slab, whose $x_3$ coordinates are $L$ and 0, are designated by $\Gamma_L$ and $\Gamma_0$ respectively. The upper semi-infinite material $M^{[0]}$, i.e. the ambient fluid (the air medium) that occupies $\Omega^{[0]}$, and $M^{[1]}$ are in firm contact through $\Gamma_L$ (i.e. the pressure and normal velocity are continuous across $\Gamma_L$ $[p(\mathbf{x})] = 0$ and $[\rho^{-1}\partial_n p(\mathbf{x})] = 0$, wherein $\mathbf{n}$ denotes the generic unit vector normal to a boundary and $\partial_n$ designates the operator $\partial_n = \mathbf{n} \cdot \nabla$).

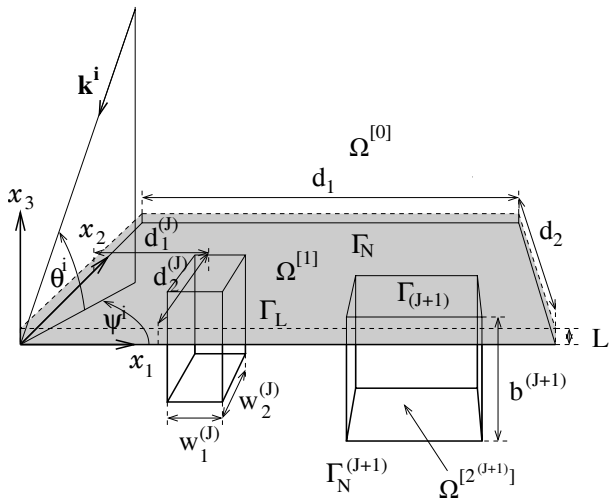


Figure 1: Representation of a **d**-periodic fluid-like porous slab backed by a rigid wall that contains periodic cubic and macroscopic irregularities excited by a plane incident wave.

The rigid backing contains cubic irregularities with period $\mathbf{d} = (d_1, d_2)$, i.e. along the $x_1$ and $x_2$ axis respectively, that create a diffraction grating. The $J$-th irregular-

ity of the unit cell occupies the cube $\Omega_{[2^{(J)}]}$ of height $b^J$ and widths $w_1^{(J)}$, $w_2^{(J)}$ along the $x_1$ and $x_2$ axis. This irregularity is occupied by a fluid material $M^{[2^{(J)}]}$. The boundary of $\Omega_{[2^{(J)}]}$ is composed of the rigid portion $\Gamma_{N^{(J)}}$ (Neumann type boundary conditions, $\partial_n p(\mathbf{x}) = 0$) and of $\Gamma_{(J)}$ through which media $M^{[2^{(J)}]}$ and $M^{[1]}$ are in firm contact (continuity of the pressure and normal velocity). The $x_1$ and $x_2$ coordinate of the center of the base segment of $\Omega_{[2^{(J)}]}$ are $d_1^{(J)}$ and $d_2^{(J)}$. $\Gamma_0$ is also composed of a rigid portion $\Gamma_N$ (Neumann type boundary conditions). The configuration is more complex than the one already studied in[1] in the sense that the structured backing is composed of a 2-dimensional grating consisting in a 2-dimensional periodic set of cubes. The method of solution, which is quite close to the one used in[1], is also briefly summarized.

We denote the total pressure, wavenumber and wave speed by the generic symbols $p$, $k$ and $c$ respectively, with $p = p^{[0]}$, $k = k^{[0]} = \omega/c^{[0]}$ in $\Omega^{[0]}$, $p = p^{[1]}$, $k = k^{[1]} = \omega/c^{[1]}$ in $\Omega^{[1]}$, and $p = p^{[2^(J)]}$, $k = k^{[2^(J)]} = \omega/c^{[2^(J)]}$ in $\Omega^{[2^{(J)}]}$.

Rather than to solve directly for the pressure $\bar{p}(\mathbf{x}, t)$ (with $\mathbf{x} = (x_1, x_2, x_3)$), we prefer to deal with $p(\mathbf{x}, \omega)$, related to $\bar{p}(\mathbf{x}, t)$ by the Fourier transform $\bar{p}(\mathbf{x}, t) = \int_{-\infty}^{\infty} p(\mathbf{x}, \omega) e^{-\mathrm{i}\omega t} d\omega$. Henceforth, we drop the $\omega$ in $p(\mathbf{x}, \omega)$ so as to denote the latter by $p(\mathbf{x})$.

The azimuth $\psi^i$ of the incident wavevector $\mathbf{k^i}$ is measured counterclockwise from the positive $x_1$ axis, while its elevation $\theta^i$ is measured counter-clockwise from the plane $x_1 - x_2$. The incident wave propagates in $\Omega^{[0]}$ and is expressed by $p^i(\mathbf{x}) = A^i e^{\mathrm{i}(k_1^i x_1 + k_2^i x_2 - k_3^{[0]i}(x_3 - L))}$, wherein $k_1^i = -k^{[0]} \cos\theta^i \cos\psi^i$, $k_2^i = -k^{[0]} \cos\theta^i \sin\psi^i$, $k_3^{[0]i} = k^{[0]} \sin\theta^i$ and $A^i = A^i(\omega)$ is the signal spectrum.

The plane wave nature of the incident wave, and the periodic nature of $\cup_{J\in\mathcal{J}} \Omega_{[2^{(J)}]}$ imply the Floquet relation

$$p(x_1 + nd_1, x_2 + md_2, x_3) = p(x_1, x_2, x_3) e^{\mathrm{i}k_1^i nd_1 + \mathrm{i}k_2^i md_2} ; \quad \forall \mathbf{x} \in \mathbb{R}^3 ; \forall (n, m) \in \mathbb{Z}^2 . \tag{1}$$

Consequently, it suffices to examine the field in the central cell of the plate which includes the cubes $\Omega^{[2^{(J)}]}$, $J \in \mathcal{J}$ in order to obtain the fields, via the Floquet relation, in the other cells.

The uniqueness of the solution to the forward-scattering problem is assured by the radiation conditions :

$$p^{[0]}(\mathbf{x}) - p^i(\mathbf{x}) \sim \text{ outgoing waves } ; \ |\mathbf{x}| \to \infty , \ x_3 > L . \tag{2}$$

## 2.2 Field representations in $\Omega^{[0]}$, $\Omega^{[1]}$ and $\Omega^{[2^{(n)}]}$

Separation of variables, the radiation conditions, and the Floquet theorem lead to the representations:

$$p^{[0]}(\mathbf{x}) = \sum_{(n,m)\in\mathbb{Z}^2} \left[ e^{-\mathrm{i}k_{3nm}^{[0]}(x_3 - L)} \delta_n \delta_m + R_{nm} e^{\mathrm{i}k_{3nm}^{[0]}(x_3 - L)} \right] e^{\mathrm{i}(k_{1n} x_1 + k_{2m} x_2)},$$
$$p^{[1]}(\mathbf{x}) = \sum_{(n,m)\in\mathbb{Z}^2} \left( f_{nm}^{[1]-} e^{-\mathrm{i}k_{3nm}^{1} x_3} + f_{nm}^{[1]+} e^{\mathrm{i}k_{3nm}^{1} x_3} \right) e^{\mathrm{i}(k_{2n} x_1 + k_{2m} x_2)}, \tag{3}$$

where $\delta_n$ is the Kronecker symbol, $k_{1n} = k_1^i + \dfrac{2n\pi}{d_1}$, $k_{2m} = k_2^i + \dfrac{2m\pi}{d_2}$, and $k_{3nm}^{[j]} = \sqrt{(k^{[j]})^2 - (k_{1n})^2 - (k_{2m})^2}$, with $\mathrm{Re}\left(k_{3nm}^{[j]}\right) \geq 0$ and $\mathrm{Im}\left(k_{3nm}^{[j]}\right) \geq 0$, $j = 0, 1$. The reflection coefficient of the plane wave denoted by the subscripts $n$ and $m$ is $R_{nm}$, while $f_{nm}^{[1]\pm}$ are the coefficients of the diffracted waves inside the slab associated with the plane wave also denoted by the subscripts $n$ and $m$.

Referring to[1], the pressure fields $p^{[2^{(J)}]}$, admits the pseudo-modal representation, that already accounts for the boundary conditions on $\Gamma_{N^{(J)}}$:

$$p^{[2^{(J)}]}(\mathbf{x}) = \sum_{(\mathcal{N},\mathcal{M})\in\mathbb{N}^2} D_{\mathcal{N}\mathcal{M}}^{[2^{(J)}]} \cos\left(k_{1\mathcal{N}}^{[2^{(J)}]} \left(x_1 - d_1^{(J)} + w_1^{(J)}/2\right)\right) \cos\left(k_{2\mathcal{M}}^{[2^{(J)}]} \left(x_2 - d_2^{(J)} + w_2^{(J)}/2\right)\right) \cos\left(k_{3\mathcal{N}\mathcal{M}}^{[2^{(J)}]} \left(x_3 + b^{(J)}\right)\right), \tag{4}$$

wherein $k_{1\mathcal{N}}^{[2^{(n)}]} = \mathcal{N}\pi/w_1^{(J)}$, $k_{2\mathcal{M}}^{[2^{(J)}]} = \mathcal{M}\pi/w_2^{(J)}$ and $k_{3\mathcal{N}\mathcal{M}}^{[2^{(J)}]} = \sqrt{(k^{[2^{(J)}]})^2 - (k_{1\mathcal{N}}^{[2^{(J)}]})^2 - (k_{2\mathcal{M}}^{[2^{(J)}]})^2}$, with $\mathrm{Re}\left(k_{3\mathcal{N}\mathcal{M}}^{[2^{(J)}]}\right) \geq 0$ and $\mathrm{Im}\left(k_{3\mathcal{N}\mathcal{M}}^{[2^{(J)}]}\right) \geq 0$, $\forall J \in \mathcal{J}$ and $D_{\mathcal{N}\mathcal{M}}^{[2^{(J)}]}$ are the coefficients of the pseudo modal representation.

# 3 Determination of the acoustic properties of the structure

## 3.1 Application of the continuity conditions across $\Gamma_L$ and $\Gamma_0$

We apply successively

- $\int_{-\frac{d_1}{2}}^{\frac{d_1}{2}} \int_{-\frac{d_2}{2}}^{\frac{d_2}{2}} \cdot \times e^{\mathrm{i}(k_{1l} x_1 + k_{2g} x_2)} dx_1 dx_2$ to the continuity i) of the pressure field and ii) of the normal component of the velocity across $\Gamma_L$ and to the continuity of iii) the normal component of the velocity across $\Gamma_N \bigcup (\bigcup_{J\in\mathcal{N}} \Gamma_{(J)})$,
- $\int_0^{w_1^{(J)}} \int_0^{w_2^{(J)}} \cdot \times \cos\left(k_{1\mathcal{P}}^{[2^{(J)}]} x_1\right) \cos\left(k_{2\mathcal{Q}}^{[2^{(J)}]} x_2\right) dx_1 dx_2$ to the continuity of the pressure field across $\Gamma_{(J)}$.

Introducing the appropriate field representation therein, Eqs.(3) and (4), and making use of orthogonality relations, give rise to the linear set of equations. After some algebra and rearrangements, this reduces to a linear system of equations for the solution of $D_{\mathcal{N}\mathcal{M}}^{[2^{(J)}]}$ which may be written in the matrix form, when denoting by $\mathbf{D}$ the infinite column matrix of components $D_{\mathcal{N}\mathcal{M}}^{[2^{(J)}]}$

$$(\mathbf{A} - \mathbf{C})\, \mathbf{D} = \mathbf{F} \tag{5}$$

where $\mathbf{F}$ is the column matrix of elements $F_{\mathcal{N}\mathcal{M}}^{(t)}$ and $\mathbf{A}$ and $\mathbf{C}$ are two square matrices of elements $A_{\mathcal{N}\mathcal{M},NM}^{(n,t)}$, and $C_{nmNM}^{(n,t)}$ respectively.

### 3.2 Evaluation of the fields

Once (5) is solved for $D^{[2^{(n)}]}_{\mathcal{NM}}$, $R_{nm}$, $f^{[1]+}_{nm}$ and $f^{[1]-}_{nm}$ in terms of $D^{[2^{(J)}]}_{\mathcal{NM}}$ can be evaluated and in particular

$$R_{nm} = \sum_{J\in\mathcal{N}} \sum_{(\mathcal{N},\mathcal{M})\in\mathbb{N}^2} \frac{\mathrm{i}w_1^{(J)}w_2^{(J)}\alpha^{[2^{(J)}]}_{nm}}{d_1 d_2 D_{nm}\alpha^{[1]}_{nm}} D^{[2^{(J)}]}_{\mathcal{NM}} \sin\left(k^{[2^{(J)}]}_{3\mathcal{NM}} b^{(J)}\right) \times I^{-(J)}_{1n\mathcal{N}} I^{-(J)}_{2m\mathcal{M}} e^{-\mathrm{i}k_{1p}\left(d_1^{(J)}-w_1^{(J)}/2\right)-\mathrm{i}k_{2p}\left(d_2^{(J)}-w_2^{(J)}/2\right)} + \delta_n\delta_m A^i \frac{\alpha^{[0]}_{nm}\cos\left(k^{[1]}_{3mn}L\right)+\mathrm{i}\alpha^{[1]}_{nm}\sin\left(k^{[1]}_{3nm}L\right)}{D_{nm}}. \quad (6)$$

Introduced in the appropriate field expression, this leads to the fields expression in each domain. These fields are expressed as a sum of i) the field in the absence of the inclusions with ii) the field due to the irregularities of the multi-component grating.

### 3.3 Evaluation of the reflection and absorption coefficients

In case of an incident plane wave with spectrum $A^i$, the conservation of energy relation takes the form

$$1 = \mathcal{A} + \mathcal{R}\,, \quad (7)$$

with $\mathcal{R}$ the hemispherical reflection defined by

$$\mathcal{R} = \sum_{(n,m)\in\mathbb{Z}^2} \frac{\mathrm{Re}\left(k^{[0]}_{3nm}\right)}{k^{[0]i}_3} \frac{\|R_{nm}\|^2}{\|A^i\|^2}\,, \quad (8)$$

wherein the expressions of $R_{nm}$ are given by Eq.(6). The absorption coefficient $\mathcal{A}$ takes the form $\mathcal{A} = \mathcal{A}_D + \mathcal{A}_S$, wherein $\mathcal{A}_D$ is the inner absorption of the domains $\Omega^{[1]}$ and $\Omega^{[2^{(J)}]}$, $\forall J \in \mathcal{J}$, and $\mathcal{A}_S$ is the surface absorption induced by the viscosity and related to the interfaces $\Gamma_L$ and $\Gamma_{(J)}$, $\forall J \in \mathcal{J}$.

In our calculations, the irregularities are filled with the air medium. Any absorption phenomenon is associated to this material, and thus the inner absorption reduces to the one of domain $\Omega^{[1]}$, and the surface absorption related to $\Gamma_{(J)}$ simplifies.

Because of the complicated shape of $\Omega^{[1]}$ and $\Omega^{[2^{(n)}]}$, but also of the non-vanishing term $\mathcal{A}_S$, $\mathcal{A}$ will not be calculated by $\mathcal{A} = 1 - \mathcal{R}$.

## 4 Numerical results, experimental validation and discussion

Numerical calculations have been performed for various geometrical parameters (couples $(d_1, d_2)$, $w_1^{(J)} \times w_2^{(J)} \times b^{(J)}$ and $(d_1^{(J)}, d_2^{(J)})$) and within the frequency range of audible sound, particularly at low frequencies. One of the main constraints in designing acoustically absorbing materials are the size and weight of the configuration. A $L = 1$ cm thick low resistivity foam (Fireflex) slab, whose parameters are reported in Table 1 was used. These parameters have been evaluated using the traditional methods described in [10].

The irregularities are filled with air, i.e. the ambient and saturating fluid ($M^{[0]}$ and $M^{[2^{(J)}]}$) is air ($\rho^{[0]} = \rho^{[2^{(J)}]} = \rho_f = 1.213$ kg m$^{-3}$, $c^{[0]} = c^{[2^{(J)}]} = \sqrt{\gamma P_0/\rho_f}$, with $P_0 = 101325$ Pa, Pr $= 0.71$, $\gamma = 1.4$, and $\eta = 1.839 \times 10^{-5}$ kg.m$^{-1}$.s$^{-1}$).

| | $\phi$ | $\alpha_\infty$ | $\Lambda$ ($\mu$m) | $\Lambda'$ ($\mu$m) | $\sigma$ (Nsm$^{-4}$) |
|---|---|---|---|---|---|
| S1 | 0.95 | 1.42 | 180 | 360 | 8900 |
| S2 | 0.99 | 1 | 70 | 210 | 7900 |

Table 1: Acoustical parameters of the porous material constituting the slab of thickness $L$.

The geometrical parameters of the configurations studied therein are:

- C1: $d_1 \times d_2 = 12 \times 8$ cm, $d_1^{(n)} \times d_2^{(n)} = 6 \times 4$ cm, $w_1^{(n)} \times w_2^{(n)} \times b^{(1)} = 6 \times 4 \times 3$ cm, $L = 1$ cm
- C2: $d_1 \times d_2 = 20 \times 8$ cm, $d_1^{(n)} \times d_2^{(n)} = 10 \times 4$ cm, $w_1^{(n)} \times w_2^{(n)} \times b^{(1)} = 12 \times 6 \times 2$ cm, $L = 1$ cm
- C3: $d_1 \times d_2 = 60 \times 60$ cm, $d_1^{(n)} \times d_2^{(n)} = 30 \times 30$ cm, $w_1^{(n)} \times w_2^{(n)} \times b^{(1)} = 30 \times 45 \times 10$ cm, $L = 2$ cm

### 4.1 One irregularity per spatial period

We shall be concerned with two cases: one in which the frequency of the fundamental Trapped mode of the Irregularity (TI) stands at lower frequency than the Modified Mode of the Boundary Layer (MMBL), and one in which the frequency of the fundamental (TI) stands at higher frequency than the modified mode of the slab (MMBL). In the first case, the MMBL would be largely excited, while in the second one, the TI would be largely excited as already noticed in[1]. The second case is obviously a particular case of the first one, the frequency of excitation of the MMBL being dependant on the angle of incidence.

Figure2a) depicts the absorption coefficient of the porous layer of characteristic S1 (see Table 1) when backed by a flat rigid backing and when backed by a rigid grating of C1 geometry. The modified modes of the slab stands at $\nu^{MMBL}_{110} \approx 2775$Hz, $\nu^{MMBL}_{101} \approx 4100$Hz, $\nu^{MMBL}_{111} \approx 6500$Hz..., while the mode of the irregularity stand at $\nu^{ti}_{000} \approx 2800$Hz, $\nu^{ti}_{010} \approx 4000$Hz, $\nu^{ti}_{001} \approx 5100$Hz... Several remarks should be made. First, $\nu^{ti}_{000}$ appears at a lower frequency than the one calculated through $\nu^{ti}_{000} = c^{[2^{(t)}]}/4b^{(t)}$ and is excited around 1900 Hz. This phenomena, already encountered in[8], is related to the boundary condition at $\Gamma_{(t)}$, which is not a Dirichlet condition but rather a continuity condition, leading to a larger effective height of the irregularity. The fundamental TI being lower than the first MMBL, the energy is advected by this mode and the associated absorption coefficient is close to unity at this frequency. The thinner is the porous layer, the closer is the fundamental TI to 2800Hz. Additional sharper peaks of absorption are noticed at higher frequencies and are associated to excitation of MMBL.

Figure2b) depicts the absorption coefficient of the porous layer of characteristic S1 when backed by a flat rigid backing and when backed by a rigid grating of C2 geometry. The modified mode of the slab stands at $\nu^{MMBL}_{110} \approx 1700$Hz, $\nu^{MMBL}_{101} \approx 4100$Hz, $\nu^{MMBL}_{120} \approx 5000$Hz..., while

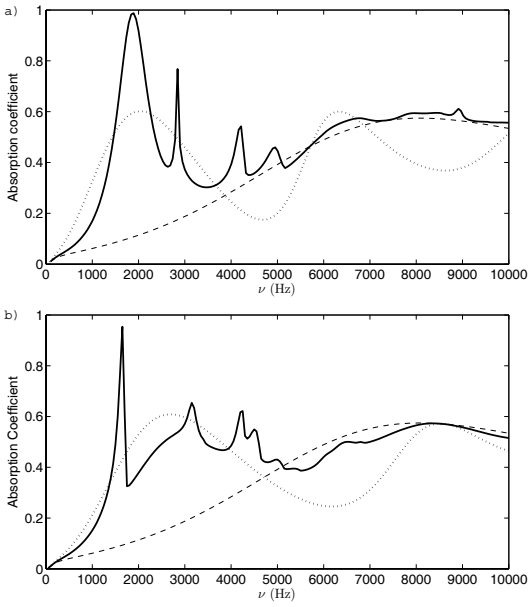


Figure 2: Absorption coefficient of a porous layer of characteristic S1 backed by a flat rigid backing (− − −) and backed by a rigid flat backing with an air layer of thickness $b^{(1)}$ in between $(\cdots)$, a) backed by an irregular rigid backing of characteristic C1 (—) and b) backed by an irregular rigid backing of characteristic C2 (—).

the fundamental trapped mode of the irregularity stand at 4275Hz. In practice, this trapped mode appears around 4100Hz. The first MMBL being lower than the fundamental TI, the energy is advected by this mode and the associated absorption coefficient is close to unity at this frequency. An additional sharper peak of absorption is noticed around 4100Hz and is associated to excitation of the second and third MMBL. The excitation of the fundamental TI leads to a smooth peak leading to an increase of the absorption around $\approx$ 3000Hz.

A particular feature is that the frequency of the fundamental TI can be correctly evaluated through the simplified problem consisting of an air layer of the same thickness as the height of the irregularity between the porous layer and a rigid flat backing. The absorption peaks associated with the fundamental TI and MMBL excitation are nevertheless higher in case of the irregular grating.

## 4.2 Experimental validation

Remarkable absorption is obtained in case of periodic irregular rigid backing, while the response of the structure without irregularities is quite well known or at least much more common. Experimental validation also focused on the periodic structure, its effect having been emphasis by comparison with the flat rigid backing in the previous numerical section.

Usually, experiments related to 1D, 2D or 3D gratings are carried out in a free field (anechoic room) and/or at higher frequencies for a finite size sample [11].

Here, we follow the idea already exploited in[1], in which the experimental validation was carried out by use of an impedance tube with a square cross section. A square cross-section impedance tube available in LAUM, 30 cm$\times$ 30 cm, whose cut-off frequency is $570Hz$, is used. This cut-off frequency corresponds to a wavelength of 60 cm.

The phenomenon related to the MMBL occurs when the wavelength is of the order of the spatial period of the grating. We also make use of the boundary conditions of the impedance tube, which are perfect mirrors below the cut-off frequency, in order to design the sample. Because of the dimensions of the impedance tube, the spatial periodicity along both $x_1$ and $x_2$ axis should be a multiple of 30 cm. If the profile of the unit cell is symmetric with regards to the axis $x_1 = d_1/2$ and $x_2 = d_2/2$, the modelled spatial period is ($d_1 \times d_2 = 60$ cm $\times$ 60 cm, as depicted in Figure 3.

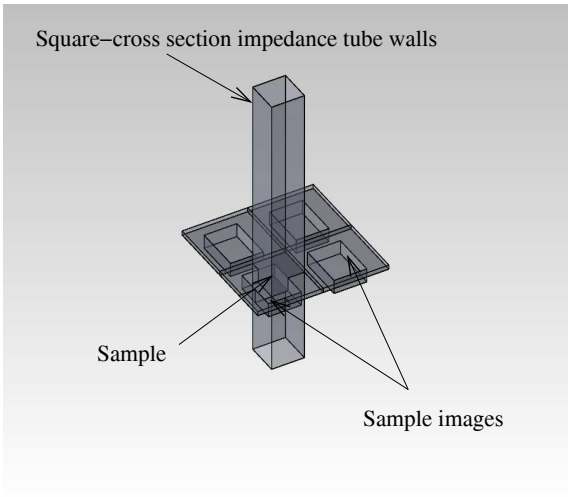


Figure 3: Cross-sectional view of the experimental set-up and sample design.

The infinitely rigid portion of the sample was made of four 1 cm thick aluminium plates, which were screwed (head screw was then filled with hard plastic silicone for the surface to be perfectly flat) in order to create a step of 10 cm height and 15 cm width along the $x_1$ and 22.5 cm width along the $x_2$. A $L = 2$ cm thick porous foam layer S2, whose characteristics are those reported in Table 1, was glued to the upper part of the step. In order to keep the porous layer flat along the step area, a screw of small diameter (3mm) was added at the edge of the lower part of the step and two nylon wires were tightened between this screw and the upper part of the step, such that the free part of the foam layer rests on it.

A comparison between the predicted et the measured absorption coefficient is plotted in Figure 4. The presented absorption coefficient is the averaged value of the absorption coefficient measured when the step of the sample lays on the bottom edge of the impedance tube and when rotated $\pi/4$. A rotation of the sample of $\pi/2$ and $3\pi/4$ is impossible in practice because the sample do not lay on the step and is no more stable in the tube.

The experimental absorption coefficient is presented for frequencies higher than 200 Hz. Below this frequency the absorption coefficient is lower than 0.1, which is limit of measurement. The two curves match well and therefore validate the present method.

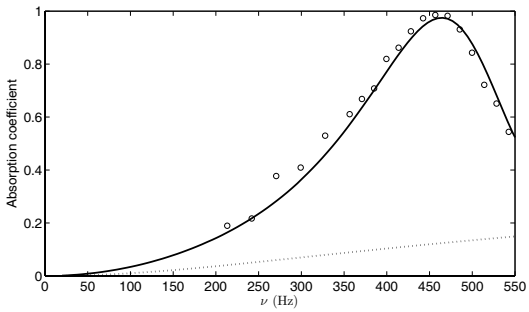


Figure 4: Comparison between the absorption coefficient of a porous layer of characteristic S2 backed by a flat rigid backing ($\cdots$) and backed by an irregular rigid backing of characteristic C3 as calculated with the present method (—) and measured experimentally (o)

# 5 Conclusions

We studied, theoretically, numerically and experimentally, the acoustic properties of a low resistivity porous layer backed by a rigid plate with periodic irregularities in the form of a grating.

We show, that the grating leads to excitation of modes, whose frequency depends both on the characteristic of the surrounding medium and of the characteristics of the porous layer and on the spatial period of the configuration $d_1 \times d_2$. These modes, whose structures are close to the one of the modes of the layer, can lead to a total absorption peak. This absorption peak occurs at the frequency of the fundamental modified mode of the layer and seems to be always a quasi-total absorption peak. The trapped mode of the irregularity also lead to quasi-total absorption peak when excited below the modified mode of the slab.

Experiments were performed in a impedance tube with square cross-section. The boundary conditions of the latter are perfect mirrors and allow us, thanks to the image theory, to model diffraction of a plane wave at normal incidence at frequencies below the cut off of the tube. Experimental results are in accordance with the theory and particularly exhibit a total absorption peak at the frequency of the fundamental modified mode of the layer.

# Acknowledgments

The authors would like to thank R. Pommier for providing us Solidworks pictures.

# References

[1] J-P Groby, W. Lauriks, and T.E. Vigran. Total absorption peak by use of a rigid frame porous layer backed with a rigid multi-irregularities grating. *J. Acoust. Soc. Am.*, 127:2865–2874, 2010.

[2] L.M. Brekovskikh. *Waves in Layered Media*. Academic Press, New-York, 1960.

[3] U. Ingard. *Notes on Sound Absorption Technology*. Noise Control Foundation, Poughkeepsie, 1994.

[4] O. Tanneau, J.B. Casimir, and P. Lamary. Optimization of multilayered panels with poroelastic components for an acoustical transmission objective. *J. Acoust. Soc. Am.*, 120(3):1227–1238, 2006.

[5] M.R. Schroeder. Toward better acoustics for concert halls. *Phys. Today*, 33:24–30, 1980.

[6] B. Sapoval, B. Hebert, and S. Russ. Experimental study of a fractal acoustical cavity. *J. Acoust. Soc. Am.*, 105:2014–2019, 1999.

[7] B. Sapoval, S. Felix, and M. Filoche. Localisation and damping in resonators with complex geometry. *Eur. Phys. J.*, 161:225–232, 2008.

[8] J-P Groby, A. Duclos, O. Dazel, L. Boeckx, and W. Lauriks. Absorption of a rigid frame porous layer with periodic circular inclusions backed by a periodic grating. *J. Acoust. Soc. Am.*, 129:3035–3046, 2011.

[9] J-P Groby, A. Duclos, O. Dazel, L. Boeckx, and L. Kelders. Enhancing absorption coefficient of a backed rigid frame porous layer by embedding circular periodic inclusions. *J. Acoust. Soc. Am.*, 130:3771–3780, 2011.

[10] J.-F. Allard. *Propagation of Sound in Porous Media: Modelling Sound Absorbing Materials*. Chapman & Hall, London, 1993.

[11] O. Umnova, K. Attenborough, and C.M. Linton. Effects of porous covering on sound attenuation by periodic arrays of cylinders. *J. Acoust. Soc. Am.*, 119:278–284, 2006.